

Surface segregation of silicon in platinum(111)

Ulrike Diebold,^{a)} Lanping Zhang, John F. Anderson, and Pawel Mrozek
Department of Physics, Tulane University, New Orleans, Louisiana 70118

(Received 2 October 1995; accepted 26 February 1996)

We present a study of an ultrathin surface layer of platinum silicide formed on a Pt(111) crystal as a result of surface segregation of Si and Ca trace impurities. The structure and composition of this surface compound is investigated with low energy He⁺ ion scattering, (LEIS), x-ray photoelectron spectroscopy (XPS), low energy electron diffraction (LEED), and scanning tunneling microscopy (STM). Si surface segregation onto Pt(111) is thermally activated; annealing at temperatures between 750 and 1100 K results in the formation of a surface silicide. The highest Si coverage that can be reached is 0.4 monolayers; the Ca coverage at saturation is below 0.02 monolayers. The enthalpy of Si segregation is found to be $-(105 \pm 30)$ kJ/mole. A well-ordered ($\sqrt{19} \times \sqrt{19}$)R23.41° or $|\begin{smallmatrix} 3 & 2 \\ -2 & 5 \end{smallmatrix}|$ structure is observed by LEED and STM; the amount of surface area covered with this structure is proportional to the Si coverage measured with LEIS. At low annealing temperatures up to 800 K, two domains coexist with $|\begin{smallmatrix} 3 & 2 \\ -2 & 5 \end{smallmatrix}|$ and $|\begin{smallmatrix} 2 & 3 \\ -3 & 5 \end{smallmatrix}|$ orientations, but only the first one is stable at Si saturation coverage. No large relaxations of substrate interatomic distances are detected upon formation of the overlayer. © 1996 American Vacuum Society.

I. INTRODUCTION

It is a well-established fact that the surface composition of multicomponent materials may be different from their bulk composition due to thermodynamically driven segregation phenomena.^{1,2} Impurity segregation towards surfaces and grain or phase boundaries is found to cause, among other things, the poisoning of industrial supported metal catalysts³ and temper embrittlement in metallurgy.¹ The driving force for this process is the decrease of the free energy of the system when the impurity atoms are moving from the bulk material to the surface. According to simple broken bond models, the segregating species has lower surface tension or lower sublimation enthalpy in the elemental state.⁴ The tendency to minimize the strain energy is also partly responsible for causing impurity surface segregation.^{4,5}

Silicon is a common impurity in high-purity platinum single crystals.⁶ Unlike other contaminants such as C, P, or Cl that are easily observed on platinum surfaces, detection of silicon is not an easy task using common surface sensitive techniques like Auger electron spectroscopy (AES)⁷ or x-ray photoelectron spectroscopy (XPS). The LMM Auger electron transitions of elemental Si or SiO₂ overlap with the platinum transitions, making the quantification uncertain. The high energy Auger *KLL* lines have low transition probabilities. The XPS sensitivity factors of the Si 2*s* and Si 2*p* photoelectron core levels are low,⁸ resulting in an intensity from a silicon monolayer of below 1% of the Pt 4*f* line intensity. In this work, we use low energy ion scattering (LEIS); with this technique, a fractional monolayer Si coverage can easily be seen.⁹ The presence of surface oxides on Pt is strongly influenced by segregation of impurities such as Si, as has been shown in detail by Salmeron *et al.*^{10–12} and others.^{9,13} More recently, it was observed that the presence of bulk impurities segregated to Pt surfaces can also significantly modify their

geometric and electronic structure. The (1×*n*), *n*=5,3, surface reconstruction correlates strongly with increasing Ca surface concentration on a Pt(110) single crystal.¹⁴ Similarly, an oxidized Si impurity stabilizes the Pt(110)(1×4) reconstruction.¹⁵ Si also prevents the thermal roughening transition of the Pt(110) surface¹⁶ and stabilizes (012) planes on a field emitter tip by preferential adsorption on the kink site.¹⁷

Segregation in platinum–silicon contacts has important practical consequences in microelectronics, materials science, and catalysis. Thorough studies of their metallurgical properties exist, particularly of the kinetics of phase formation and microstructures.^{18,19} The electronic structure at the platinum silicide silicon interface was studied using electron spectroscopy techniques.^{20,21} Atom probe FIM studies showed that platinum silicide layers grow epitaxially on the Pt(111) plane at 1073 K and that the silicide layers adjacent to the substrate have a Pt₂Si composition.²² Although the silicide–metal interface is sharp, Si atoms are very mobile and tend to diffuse deep into the platinum substrate at ~1073 K.²² For evaporated Pt layers on Si the initial phase formed at low Pt coverages is PtSi with a small Pt₂Si component.²³

Despite this fundamental and technological interest in the interaction of silicon and platinum at surfaces, only few detailed investigations of Si segregation on single-crystalline surfaces exist. Cardillo and Becker²⁴ studied Si segregation onto a Pt(100) surface and observed an ordered structure that was assigned to formation of a Pt₂Si(100) overlayer with one monolayer (1 ML) thickness. On Pt(111), Si segregation was observed previously,^{9,12,13} but no detailed structural and compositional investigations have been reported. In this work, we find that a surface compound containing ~40 at. % of Si is formed through thermally activated Si segregation on a Pt(111) crystal with a few ppm Si bulk impurity. The segre-

^{a)}Electronic mail: diebold@mailhost.tcs.tulane.edu

gated layer is up to 1–2 ML thick and exhibits a stable $(\sqrt{19} \times \sqrt{19})R23.41^\circ$ structure with well defined long-range order.

II. EXPERIMENT

Experiments are performed in ultrahigh vacuum with a base pressure of 3×10^{-11} mbar equipped for XPS, LEIS, low energy electron diffraction (LEED), and scanning tunneling microscopy (STM). The LEIS and XPS measurements are conducted using a cylindrical sector analyzer. The sample is heated indirectly and temperature measurements are performed by a Chromel–Alumel thermocouple attached to the sample holder. The estimated uncertainty in the temperature measurement is ± 16 K; the sample cooling rate is around 1 K/s. The LEED measurements are conducted using a reverse view LEED system. Our STM results are obtained using a commercial scanning tunneling microscope (Omicron UHV STM-1) operated in the constant current mode. STM tips are electrochemically etched from a tungsten wire and occasionally cleaned in vacuum by voltage pulses up to 10 V while tunneling. The STM images are constant current topographies.

The Pt(111) single crystal used was an 8-mm-diam disk of 1 mm thickness oriented by Laue diffraction within 1° and mechanically polished with diamond paste (from Buehler) down to 0.25 μm grade. This crystal carries relatively high quantities (few ppm) of Si and Ca bulk impurities, which segregate towards the surface during annealing. As a reference, a second Pt(111) crystal showing no Si contamination is also examined. Initially, both samples showed small amounts of carbon impurity. For initial treatment, we used a cleaning procedure recently reported²⁵ involving multiple cycles of 600 eV Ar^+ sputtering at 910 K and sample annealing at 880 K in 2×10^{-6} mbar of oxygen. The last step was annealing at 1100 K for 10 min. This procedure was effective in removing the carbon impurity.

For studying the segregation behavior of Si and Ca towards the surface of the Pt(111) crystal containing high amounts of bulk impurities, the sample was sputter cleaned using 600 eV Ar^+ at room temperature for 30–60 min. This reduces the Si and Ca signals below the detection limit for LEIS and XPS. Usually, sputtering induces a compositional change that is limited to an altered layer with a thickness of a few tens of nanometers; thus, the mean silicon bulk concentration is not affected. The Pt(111) single crystal freshly prepared by sputtering is then annealed in ultrahigh vacuum at elevated temperatures for 1–1.5 h to force impurity surface segregation. Ion scattering measurements (1225 eV He^+ ion beam, 20 nA, scattering angle 137°) are performed during annealing as well as at room temperature. The elemental sensitivities of Si and Pt are determined in a separate experiment using Si(111) and Pt(111) reference samples. The sensitivity factor ratio of silicon to platinum for our experimental setup is 0.09, which is close to the value of 0.14 reported by Taglauer.²⁶ XPS measurements are completed during sample cooling; STM and LEED studies are done at room temperature.

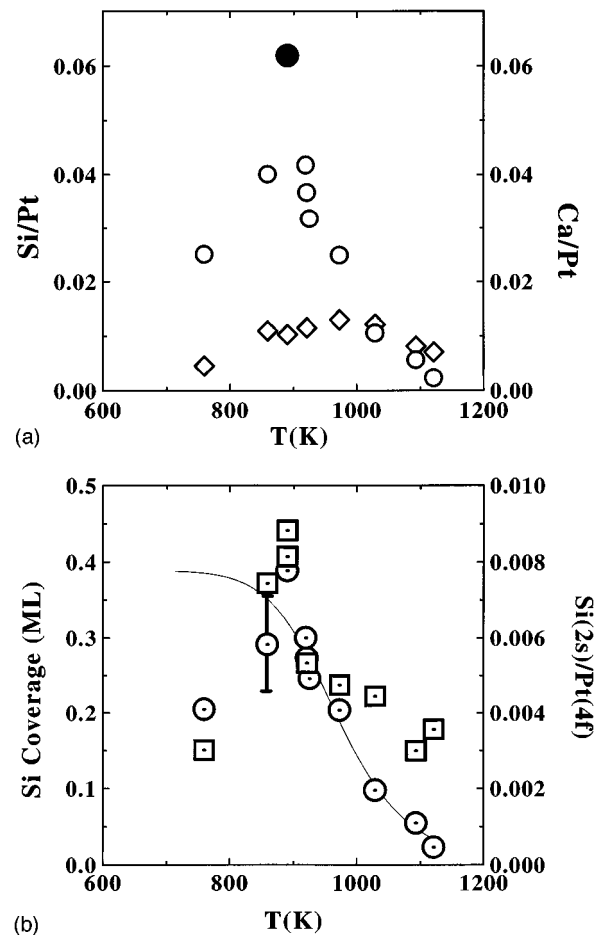


Fig. 1. (a) Evolution of LEIS intensities as a function of temperature: Si/Pt: circles (left axis); Ca/Pt: diamonds (right axis). The data point at 890 K results from a "forced segregation" experiment (see the text). (b) Evolution of silicon coverages (in monolayers) on Pt(111) as a function of temperature. Si coverage from LEIS: circles (left axis); Si 2s/Pt 4f photoelectron intensity ratio: squares (right axis). The solid line is to guide the eye.

III. RESULTS

The evolution of Si and Ca intensities segregated to the Pt(111) surface as a function of annealing temperature is shown in Fig. 1(a); the LEIS data shown are taken at specified temperature. The amount of segregated Si increases with temperature, reaches a maximum round 900 K, and then decreases. The disappearance of segregated species from the surface at high temperatures is expected from the Langmuir–McLean adsorption isotherm. Below 900 K, the annealing time was not long enough to reach thermodynamic equilibrium; therefore, intensities are lower. The data point ascribed to 890 K is the result of a different annealing procedure. After room temperature sputtering, the sample temperature was brought to 1100 K and then decreased to 700 K, in steps of 50 K. Each temperature was maintained for 12 min; subsequently, the sample was cooled down to room temperature. This "forced" segregation treatment generates a Si coverage of 0.4 ML (see below), which corresponds to the highest coverage that can be achieved at thermodynamic equilibrium. The Ca coverage is nearly constant in the range of

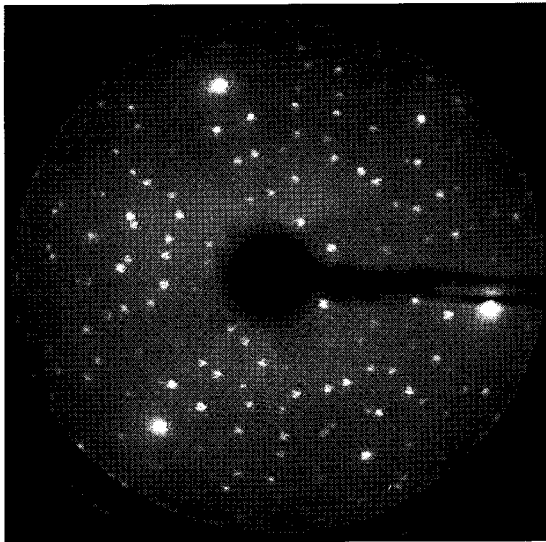


Fig. 2. $(\sqrt{19} \times \sqrt{19})R23.41^\circ$ or $|\begin{smallmatrix} -3 & 2 \\ -2 & 5 \end{smallmatrix}|$ LEED pattern after prolonged annealing of Pt(111), electron energy 84.5 eV.

temperatures studied and starts to decrease above 1050 K. Despite the clear signal in LEIS, no Ca could be detected in XPS; the Ca coverage on the sample must be below the estimated XPS sensitivity of 0.02 Ca monolayers of our experimental setup.

In Fig. 1(b) we present silicon coverages on the Pt(111) crystal derived from experimental LEIS intensity ratios [see Fig. 1(a)], and Si 2*s*/Pt 4*f* XPS intensity ratios. Both sets of results show similar behavior as a function of temperature, with a sharp maximum round 900 K. Above 1000 K, the Si coverages measured by ion scattering are lower than the values from XPS. This can be explained by the fact that the ion scattering results taken at high temperatures give the actual (low) Si surface coverage, as expected from the Langmuir–McLean isotherm. The photoelectron intensities, on the other hand, are measured at room temperature; because of our finite sample cooling rate, the system is frozen at a state corresponding to a temperature somewhat lower than the annealing temperature. Segregation is already kinetically limited below 900 K, so the “freezing” temperature must be around this value. The measured binding energies of the silicon core levels, $E_B(\text{Si } 2p) = 100.4 \pm 0.15$ eV and $E_B(\text{Si } 2s) = 151.4 \pm 0.15$ eV suggest Pt₂Si or PtSi formation. The literature value for platinum silicides is 100.5 eV⁸ for Si 2*p*.

After a “forced” surface segregation treatment, an electron diffraction pattern with striking long range order is observed (Fig. 2). this structure is identified as $(\sqrt{19} \times \sqrt{19})R23.41^\circ$, or more exactly as $|\begin{smallmatrix} -3 & 2 \\ -2 & 5 \end{smallmatrix}|$ after Schardt and Tiessen.²⁷ This pattern shows similar positions of the integral spots as the (1×1)-Pt(111) structure prepared by Ar⁺ sputtering. Thus, no large relaxation of substrate interatomic distances takes place upon overlayer formation. A $(\sqrt{19} \times \sqrt{19})R23.41^\circ$ has been observed after annealing a Pt(111) crystal with Ca contamination in oxygen.¹¹ The pattern was assigned as a CaO(111) overlayer on the Pt(111) surface. Our

sample was annealed in ultrahigh vacuum (UHV) with negligible oxygen adsorption from the residual gas within the time scale of the experiment; thus, we can exclude CaO formation as an interpretation for our results. In order to check if Si or Ca are responsible for the superstructure, we examined a second crystal that contained a comparable Ca content but no Si. Even after prolonged annealing, we did not observe any overlayer structure in LEED or STM. Figure 3(a) shows a wide-area STM image after sputtering, annealing to 740 K for 10 min, and cooling down to room temperature. A clear hexagonal superstructure is visible on the surface, arranged in islands of different sizes. The enhanced contrast at the step edges is an effect of the background subtraction routine. Note that annealing to 740 K is within the temperature range where segregation is still kinetically limited. The fraction of the surface covered with the hexagonal pattern correlates with the intensities of Si LEIS and XPS signals, with full coverage for “forced” segregation. Since the Ca coverage is rather small (below 0.02 ML), we ascribe the distinct hexagonal pattern to the presence of Si at the surface.

Figure 3(b) shows a small-area image of two domains of the hexagonal structure. The lattice constant of the unit cell is 11 Å, somewhat smaller than the 12.1 Å expected from the $(\sqrt{19} \times \sqrt{19})R23.41^\circ$ structure observed with LEED. In the simplest model of the surface structure, the bright corners of the unit cell are ascribed to single atoms or groups of atoms protruding from the surface, Fig. 3(c). If these atoms are placed into threefold hollow sites of the Pt(111) lattice, two different orientations are possible. These correspond to $|\begin{smallmatrix} -3 & 2 \\ -2 & 5 \end{smallmatrix}|$ and $|\begin{smallmatrix} -2 & 2 \\ -3 & 5 \end{smallmatrix}|$ structures built on a Pt(111) crystal. For annealing temperatures where only part of the surface is covered, we observe that a small fraction of islands consists of the rotated domain. For full coverage, only the $|\begin{smallmatrix} -3 & 2 \\ -2 & 5 \end{smallmatrix}|$ structure is visible, suggesting that the rotated orientation is metastable and transforms into the more stable $|\begin{smallmatrix} -3 & 2 \\ -2 & 5 \end{smallmatrix}|$ structure at higher annealing temperature and coverages. The contrast within the unit cell changes when changing the tunneling voltage suggesting a nonuniform composition. The corners of the surface unit cell appear bright in all images, independent of the tunneling voltage corroborating our assumption of a buckled surface.

IV. DISCUSSION

It is frequently reported that two stable platinum silicide phases, PtSi and Pt₂Si, exist.²⁸ Are any of these phases formed on the surface of a Pt(111) single crystal? The chemical shifts observed for the Si core levels strongly suggest that platinum silicide formation is indeed occurring upon Si segregation. The distinct structure observed with STM at all coverages is indicative of strong Pt–Si interatomic interactions. Cardillo and Becker report formation of an ordered Pt₂Si surface on Pt(100) formed from a trace Si impurity.²⁴ Epitaxial growth of Pt₂Si on Pt(111) was convincingly shown by Tsong using atom probe FIM.²² Our own experimental value for the Pt:Si composition at the highest coverage reached is somewhat lower than expected for a 2:1 stoichiometry. For the sake of further analysis, we assume that a

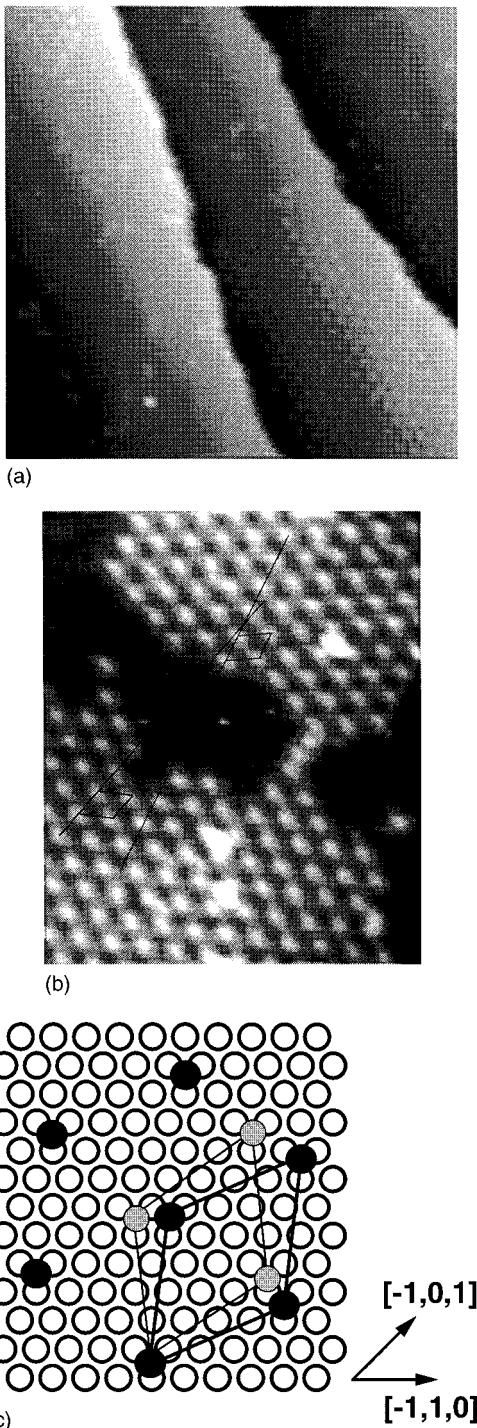


FIG. 3. (a) Large-area STM topography, $30 \text{ nm} \times 30 \text{ nm}$, sample bias voltage -0.46 V , tunneling current 0.48 nA . The Pt(111) crystal was annealed at 740 K for 10 min and subsequently cooled to room temperature. (b) STM topography of domain structure, $13 \text{ nm} \times 15 \text{ nm}$, sample bias voltage 0.46 V , tunneling current 0.53 nA . The Pt(111) crystal was annealed at 740 K for 10 min and subsequently cooled to room temperature. The unit cells of the two domains are indicated. (c) Unit cell structures for $\sqrt{19}$ domains superimposed onto a Pt(111) mesh.

Pt_2Si compound is formed on the Pt(111) surface. From examination of angular-dependent Pt $4f$ and Si $2s$ photoelectron intensities after a “forced” segregation experiment, we estimate the thickness of this compound to be $1\text{--}2 \text{ ML}$.

Based on various segregation theories,^{4,5} Si tends to segregate towards the surface of dilute Pt(Si) alloys. For the simple case of a diluted binary alloy and noninteracting species, surface segregation can be described using the Langmuir–McLean isotherm. When LEIS intensities from Fig. 1(a) are evaluated according to this isotherm, a segregation enthalpy of $-(105 \pm 30) \text{ kJ/mol}$ is derived; somewhat lower values have been obtained by others using a similar procedure.^{9,12} The enthalpy of segregation includes energy contributions from the enthalpy of solution, the difference of surface energies of the pure materials, and the elastic size mismatch energy.⁴ The difference between the sublimation enthalpies of Si and Pt is -107 kJ/mol ,²⁹ strongly favoring Si segregation in ideal solution or regular solution approximations. When we calculate the enthalpy of segregation according to Miedema,⁵ the result is -77 kJ/mol , describing a pronounced segregation of Si.

Segregation enthalpies obtained by applying the Langmuir–McLean isotherm for analysis of experimental data have to be taken with some caution, since this model describes segregation of noninteracting species and deviations are expected for strong interatomic interaction.³⁰ Long- and short-range order phenomena have been shown to lead to ordered phases on surfaces and to affect the extent of surface segregation.³¹ However, based on some qualitative considerations, we believe that the value of -105 kJ/mol is justified. Silicide formation is an exothermic reaction with a heat of formation of -67 kJ/mol for PtSi and -43.5 kJ/mol for Pt_2Si .³² As expected for intermetallic compounds, our result for the segregation enthalpy -105 kJ/mol , is mainly due to the big difference in sublimation enthalpies and is high in comparison with the formation enthalpies. Similarly,¹ this value is close to the heat of solution of Si in Pt, -138 kJ/mol .²¹

One can think of two mechanisms for Si segregation, diffusion via a vacancy mechanism in the diluted PtSi alloy, and diffusion along dislocations and grain boundaries. The activation energy for Si self-diffusion in PtSi has been determined as 200 kJ/mol .³³ Si diffusion fed from distorted sites at grain boundaries in aluminum has an activation energy of 66 kJ/mol .³⁴ Since silicon solubility at grain boundaries is probably higher than in the bulk Pt crystal (around 1.4 at. \% of Si in Pt²⁸), defects on grain boundaries saturated with Si act most likely as a source of Si for surface segregation.

V. CONCLUSIONS

We have found that pronounced Si impurity segregation in Pt(111) leads to the formation of a platinum silicide compound; the maximum thickness of this compound is $1\text{--}2 \text{ ML}$. A $(\sqrt{19} \times \sqrt{19})\text{R}23.41^\circ$ structure is observed as surface termination; the surface area covered by islands of this symmetry scales with the Si surface coverage. Two ordered domains, $|\begin{smallmatrix} -3 & 2 \\ -2 & 3 \end{smallmatrix}|$ and $|\begin{smallmatrix} -3 & 3 \\ -2 & 3 \end{smallmatrix}|$, with unit cell constants of 11 \AA are found at low Si coverages and at low segregation temperatures up to 800 K . At higher silicon coverages, only the $|\begin{smallmatrix} -3 & 2 \\ -2 & 3 \end{smallmatrix}|$ domain is observed, proving it to be a stable structure.

Using a Langmuir–McLean isotherm, we have determined the segregation enthalpy as $-(105 \pm 30)$ kJ/mol.

ACKNOWLEDGMENTS

This work is supported in part by the Louisiana Board of Regents through the Louisiana Education Quality Support Fund LEQSF (1994–97)-RD-A-26 and by the Donors of The Petroleum Research Fund, administered by the American Chemical Society, as well as DOE-EPSCOR. The authors thank Dr. Alan Burns, Sandia National Laboratory, for lending them a Pt crystal.

¹*Interfacial Segregation*, edited by W. C. Johnson and J. M. Blakely (American Society for Metals, Metals Park, OH, 1977).

²*Surface Segregation Phenomena*, edited by P. A. Dowben and A. Miller (Chemical Rubber, Boca Raton, FL, 1990).

³G. A. Somorjai, *Surf. Sci.* **299/300**, 849 (1994).

⁴F. L. Williams and D. Nason, *Surf. Sci.* **45**, 377 (1974).

⁵A. R. Miedema, *Z. Metallk.* **69**, 455 (1978).

⁶R. G. Musket, W. McLean, C. A. Colmenares, D. M. Makowiecki, and W. J. Siekhaus, *Appl. Surf. Sci.* **10**, 143 (1982).

⁷M. Mundschau and R. Vanselow, *Surf. Sci.* **157**, 87 (1985).

⁸J. F. Moulder, W. F. Stickle, P. E. Sobol, and K. D. Bomben, *Handbook of X-ray Photoelectron Spectroscopy* (Perkin-Elmer, Physical Electronics Division, Eden Prairie, MN, 1992).

⁹H. P. Bonzel, A. M. Franken, and G. Pirug, *Surf. Sci.* **104**, 625 (1981).

¹⁰M. Salmerón and G. A. Somorjai, *Surf. Sci.* **91**, 373 (1980).

¹¹M. Salmerón, L. Brewer, and G. A. Somorjai, *Surf. Sci.* **112**, 207 (1981).

¹²M. Salmerón and G. A. Somorjai, *J. Vac. Sci. Technol.* **19**, 722 (1981).

¹³H. Niehus and G. Comsa, *Surf. Sci.* **102**, L14 (1981).

¹⁴M. Stock, J. Risse, U. Korte, and G. Meyer-Emsen, *Surf. Sci.* **233**, L243 (1990).

¹⁵W. Thale, U. Korte, and G. Meyer-Emsen, *Surf. Sci.* **276**, L19 (1992).

¹⁶R. Vanselow, *Surf. Sci. Lett.* **279**, L213 (1992).

¹⁷R. Vanselow and M. Mundschau, Proceedings of the 9th Seminar on Surface Physics, Wroclaw, Poland, 1985 [Proc. Acta Universitatis Wratislaviensis, p. 937 (1985)].

¹⁸J. B. Bindell, J. W. Colby, D. R. Wonsidler, J. M. Poate, D. R. Conley, and T. C. Tisone, *Thin Solid Films* **37**, 441 (1967).

¹⁹R. D. Thompson and K. N. Tu, *Thin Solid Films* **93**, 265 (1982).

²⁰G. Rossi, I. Abbati, L. Braicovich, I. Lindau, W. E. Spicer, *Phys. Rev. B* **25**, 3627 (1982).

²¹M. del Giudice, J. J. Joyce, and J. H. Weaver, *Phys. Rev. B* **36**, 4761 (1987).

²²T. T. Tsong, *Mater. Res. Soc. Symp. Proc.* **25**, 363 (1984).

²³R. J. Nemanich, C. C. Tsai, B. L. Stafford, J. R. Abelson, and T. W. Sigmon, *Mater. Res. Soc. Symp. Proc.* **25**, 9 (1984).

²⁴M. J. Cardillo and G. E. Becker, *Surf. Sci.* **99**, 269 (1980).

²⁵T. Michely and G. Comsa, *Surf. Sci.* **256**, 217 (1991).

²⁶E. Taglauer, in *Ion Spectroscopies for Surface Analysis*, edited by A. W. Czanderna and D. M. Hercules (Plenum, New York, 1991), p. 363.

²⁷B. Schardt and H. Tiessen, Atlas of LEED Structures (unpublished).

²⁸M. Hansen and K. Anderko, *Constitution of Binary Alloys* (McGraw-Hill, New York, 1958).

²⁹*Metals Reference Book*, edited by C. J. Smithells and E. C. Brandes (Butterworths, London, 1976).

³⁰I. Jäger, *Surf. Sci.* **331–333**, 156 (1995).

³¹P. Mrozek and A. Jablonski, *Surf. Sci.* **208**, 351 (1989).

³²M. Schluter, *Thin Solid Films* **93**, 3 (1982).

³³A. P. Botha, S. Kritzing, and R. Pretorius, *Thin Solid Films* **141**, 41 (1986).

³⁴D. Aberdam, C. Corotte, and D. Dufayard, *Surf. Sci.* **133**, 114 (1983).